ANTIOXIDANTS & REDOX SIGNALING
Volume 11, Number 4, 2009

DOI: 10.1089/ars.2008.2155

Original Research Communication

Sulfaphenazole Protects Heart Against Ischemia–Reperfusion Injury and Cardiac Dysfunction by Overexpression of iNOS, Leading to Enhancement of Nitric Oxide Bioavailability and Tissue Oxygenation

Mahmood Khan,[1] Iyyapu K. Mohan,[1] Vijay K. Kutala,[1] Sainath R. Kotha,[2] Narasimham L. Parinandi,[2] Robert L. Hamlin,[3] and Periannan Kuppusamy[1]

Abstract

The objective of this study was to establish the cardioprotective effect of sulfaphenazole (SPZ), a selective inhibitor of cytochrome P450 2C9 enzyme, in an *in vivo* rat model of acute myocardial infarction (MI). MI was induced by 30 min ligation of left anterior descending coronary artery, followed by 24 h reperfusion (I/R). The study used 6 groups: I/R (control); SPZ; L-NAME; L-NAME + SPZ; 1400W (an inhibitor of iNOS); 1400W + SPZ. The agents were administered orally through drinking water for 3 days prior to induction of I/R. Myocardial oxygenation (pO_2) at the I/R site was measured using EPR oximetry. The preischemic pO_2 value was 18 ± 2 mm Hg in all groups. At 1 h of reperfusion, the SPZ group showed a significantly higher hyperoxygenation when compared to control (45 ± 1 *vs.* 34 ± 2 mm Hg). The SPZ group showed a significant improvement in the contractile functions and reduction in infarct size. Histochemical staining of SPZ-treated hearts exhibited significantly lower levels of superoxide and peroxynitrite, and markedly increased levels of iNOS activity and nitric oxide. Western blot analysis indicated upregulation of Akt and attenuation of p38MAPK activities in the reperfused myocardium. The study established that SPZ attenuated myocardial I/R injury through overexpression of iNOS, leading to enhancement of nitric oxide bioavailability and tissue oxygenation. *Antioxid. Redox Signal.* 11, 725–738.

Introduction

Acute myocardial infarction (MI) occurs when the blood supply to a region of the heart is interrupted, most commonly due to rupture of a coronary plaque. The resulting ischemia or oxygen deprivation, if left untreated, can cause damage and death of heart muscle. Unfortunately, reintroduction of blood flow to the ischemic tissue can also cause tissue damage, termed as reperfusion injury. The pathogenesis of myocardial ischemia–reperfusion (I/R) injury is known to involve interplay of multiple mechanisms. Several studies have implicated reactive oxygen species (ROS), including superoxide radical ($O_2^{-\cdot}$), hydrogen peroxide (H_2O_2), hydroxyl radical ($^{\bullet}OH$), and peroxynitrite ($ONOO^-$) that are generated upon reperfusion, in the I/R-mediated oxidative damage to the myocardium (25). The involvement of ROS in mediating I/R injury has been established based on the efficacy of antioxidants and free radical scavengers, such as superoxide dismutase (SOD), catalase, melatonin, and vitamin E, in minimizing I/R injury (12). Overexpression of manganese SOD (MnSOD), copper–zinc SOD (CuZnSOD), or glutathione peroxidase has been reported to protect the heart from I/R injury, further supporting the involvement of ROS in the reperfusion injury (8, 9, 65).

Unlike ROS, the involvement of nitric oxide (NO) in I/R injury has been controversial. NO, which is produced by a

Davis Heart and Lung Research Institute, Divisions of [1]Cardiovascular Medicine and [2]Pulmonary and Critical Care Medicine; Departments of Internal Medicine; and [3]Department of Veterinary Biosciences, The Ohio State University, Columbus, Ohio.

variety of mammalian cells, is an important mediator of both physiological and pathological vascular functions (37, 43). NO production is catalyzed by nitric oxide synthase (NOS). Enhanced NO generation was observed in the heart during I/R (13, 69). Decrease of NO production using NOS-inhibitors showed a decrease in the I/R-mediated functional impairment of the heart (44, 64). However, NO has also been shown to play a cardioprotective role in myocardial I/R injury (28, 36, 48, 54, 57, 63). Supplementation with L-arginine (substrate for NO production by NOS) and NO donors during reperfusion has been shown to be cardioprotective in regional, as well as in global ischemic models (36, 57, 63).

The cytochrome P450 (CYP) family of enzymes plays a significant role in normal cardiovascular homeostasis, as well as in cardiovascular pathogenesis (26). Particularly, CYP 2C9 has been implicated in myocardial I/R injury (23, 45, 55). CYP 2C9 has been identified as a potent source of superoxide radicals in the reperfused heart (18, 23, 45, 55). A role for CYP 2C9 in myocardial I/R injury was first demonstrated by Granville *et al.* (23) in an isolated rat heart model using CYP 2C6/9 inhibitors such as chloramphenicol, sulfaphenazole (SPZ), and cimetidine. The CYP 2C6/9 inhibitors were found to markedly attenuate infarct size and creatine kinase release. Superoxide was also found to be significantly reduced, while postischemic coronary flow was increased in the CYP inhibitor-treated hearts, indicating that NO scavenging and oxidative damage are likely to play a role in the protection against I/R-induced injury (23). These results were also reproduced in a rabbit coronary artery ligation model of focal I/R injury (23). A recent clinical study showed that SPZ could improve endothelium-dependent, NO-mediated vasodilation in patients with coronary artery disease (CAD) as assessed by increased acetylcholine-induced forearm blood-flow compared with control patients (17). The beneficial effect of SPZ administration was attributed to an increase in the bioavailability of NO in tissue and circulation during reperfusion. Similarly, a more recent study using SPZ administration in diabetic mice exhibited restoration of endothelium-dependent vasodilation, possibly by decreasing superoxide levels (14). However, the exact mechanism by which SPZ attenuates myocardial injury is not well understood.

Our recent study using isolated rat hearts showed that SPZ protected the hearts from I/R injury by scavenging ROS and increasing NO levels (31). However, it was not clear whether the increased NO levels in the SPZ-treated I/R-hearts were due to SPZ-mediated superoxide depletion or activation of endogenous pathways of NO production. This led us to hypothesize that SPZ may, in addition to inhibition and/or scavenging of superoxide generation, induce NO generation by activating endogenous inducible NOS (iNOS) in the reperfused heart. The elevated levels of NO bioavailability in the reperfused heart could have profound effects on the oxidative/nitrative stress, tissue oxygenation, infarction, and functional recovery. Therefore, the overall aim of this study was to investigate the cardioprotective effect of SPZ and to delineate the involvement of NO, superoxide, oxygenation and also to establish the signaling mechanism involved in cardioprotection in an *in vivo* rat model of acute myocardial infarction. The results from the present study showed that pretreatment of rats with SPZ significantly attenuated superoxide levels and induced iNOS expression in the reperfused heart with a concomitant enhancement of NO bioavailability and tissue oxygenation, leading to the improved recovery of cardiac function *in vivo*.

Materials and Methods

Chemicals

Sulfaphenazole [SPZ, 4-amino-N-(1-phenyl-1*H*-pyrazol-5-yl)], N^{ω}-nitro-L-arginine methyl ester (L-NAME), dihydroethidium (DHE), 2,3,5-triphenyltetrazolium chloride (TTC), and monoclonal anti-β-actin antibody were obtained from Sigma (St. Louis, MO). 4-Amino-5-methylamino-2′,7′-difluorofluorescein (DAF-FM) diacetate was obtained from Invitrogen (Carlsbad, CA). Polyclonal anti-iNOS antibody was procured from Santa Cruz Biotechnology (Santa Cruz, CA). Rabbit immuno-affinity-purified anti-nitrotyrosine antibody was obtained from Upstate Biotechnology (Lake Placid, NY). Phospho-specific antibodies for Akt, ERK1/2, and p38 MAPK were obtained from Cell Signaling (Beverly, MA). Horseradish peroxidase-conjugated secondary antibodies were obtained from Amersham Biosciences (Piscataway, NJ). Peroxynitrite was from Upstate Chemicals (Pickens, SC). Lithium octa-*n*-butoxy-naphthalocyanine (LiNc-BuO) oximetry probe was synthesized as reported (47).

Experimental protocol

Male Sprague–Dawley rats (250–300 g) were used in this study. Rats were randomly divided into six groups: I/R (control); SPZ (300 μM); L-NAME (100 μM); SPZ + L-NAME (300/100 μM); 1400W (1 mg/kg b.w.); 1400W+SPZ. The animals were treated with the drugs in drinking water for 3 days prior to experimentation. The rats consumed a daily average of 30 ml water containing 300 μM SPZ and/or 100 μM L-NAME, which is equivalent to 8.1 mg/kg b.w. of SPZ and/or 2.3 mg/kg b.w. of L-NAME 1400W was administered i.p. 30 min prior to the induction of I/R. Ischemia was induced by temporarily ligating the left anterior descending coronary artery (LAD) for 30 min, followed by reperfusion for 1 or 24 h by releasing the ligation. Myocardial tissue pO_2 at the ischemic site was continuously monitored during the ischemia–reperfusion period up to 1 h, and then at 24 h of reperfusion. Left ventricular contractile functions were measured at 24 h of reperfusion. Superoxide and nitric oxide levels in the excised heart tissue at 10 min of reperfusion were determined by histochemical staining and fluorescence microscopy. Myocardial infarct size and immunohistochemical staining for iNOS and peroxynitrite were performed on excised heart tissues after 24 h of reperfusion. All the procedures were performed with the approval of the Institutional Animal Care and Use Committee of the Ohio State University and conformed to the Guide for the Care and Use of Laboratory Animals (NIH Publication No. 86-23).

Induction of myocardial I/R injury

Rats were anesthetized with ketamine (50 mg/kg, i.p.) and xylazine (5 mg/kg, i.p.) followed by isoflurane (1–20%) with air. MI was induced by ligating the left anterior descending coronary artery (LAD), as described (5, 50). An oblique 12 mm incision was made 8 mm away from the left sternal border toward the left armpit. The chest cavity was opened with scissors by a small incision (10 mm length) at the level of the third or fourth intercostal space, 3–4 mm from the left sternal border. The LAD was visualized as a pulsating bright red

spike, running through the midst of the heart wall from underneath the left atrium toward the apex. The LAD was ligated 2–3 mm below the tip of the left auricle, using a tapered needle and a 6-0 polypropylene ligature. The ligature was passed underneath the LAD and a double knot was made to occlude the coronary artery. Occlusion was confirmed by the sudden change in color (pale) of the anterior wall of the left ventricle (LV). The ligature was released after 30 min of ischemia, and the chest cavity was closed by tying together the 4^{th} and 5^{th} ribs with one 4-0 silk suture. The layers of muscle and skin were closed with a 4-0 polypropylene suture. After LAD ligation, successful infarction was confirmed by an ST elevation on electrocardiograms that were recognized in all rats. After 30 min, the ligation was released, and the chest was closed. After resuming spontaneous respiration, animals were extubated and allowed to recover in a warm cage.

Measurement of mean arterial blood pressure (MABP)

The MABP at baseline, ischemia (30 min), and during reperfusion (1 h) was measured by inserting a microtip transducer catheter (SPR-1000, ADInstruments, Colorado Springs, CO) into the right carotid artery. The catheter was connected to a computer-based data acquisition system (PowerLab, ML866, ADInstruments) for continuous monitoring of MABP and heart rate.

Measurement of cardiac contractile functions

Cardiac contractile functions were measured in rats anaesthetized using pentobarbital sodium (50 mg/kg) at 24 h of reperfusion. A Millar catheter (SPR-1000) was advanced through the right carotid artery into the LV. The LV systolic pressure (LVSP), and maximum rate of increase (dP/dt_{max}) and decrease (dP/dt_{min}) of LV pressure were recorded and analyzed using PowerLab.

Measurement of myocardial infarction

After 24 h reperfusion, rats were reintubated and ventilated as mentioned above, the LAD was reoccluded, and 0.2 ml of 2.0% Evans blue was injected from the inferior vena cava to delineate the nonischemic myocardial tissue. The animals were sacrificed immediately and their hearts were then cut into four transverse slices. The tissue slices were incubated at 37°C for 10 min with a 1.5% solution of TTC in PBS to determine the infarct area and the area at risk (AAR). Images were captured digitally under a dissecting microscope. LV area, AAR, and infarct area were determined by computerized planimetry using MetaVue image analysis software (Molecular Devices, Downingtown, PA). The areas of myocardial tissue showing white and red colorations were defined as the regions of infarct and AAR, respectively, and the infarct size was determined. Infarct size was expressed as percentage of AAR.

Measurement of myocardial pO_2 using in vivo *EPR oximetry*

Myocardial pO_2 was measured using our established EPR oximetry method (47). The principle of EPR oximetry is based on molecular oxygen-induced line-width changes in the EPR spectrum of a paramagnetic probe. The probe usually is a microcrystal of stable nontoxic paramagnetic material that can be permanently implanted in the tissue region of interest using a 25-gauge surgical needle. Immediately following implantation, the probe responds to pO_2 in the immediate microenvironment, mostly at the crystal–tissue interface, enabling magnetic resonance-based noninvasive and repeated measurements of pO_2 for a prolonged period, months to years, from the same site. The technology has been well established and validated for measurements of pO_2 from single cells to whole organs (30, 35, 47). To our knowledge, this is the first report on the use of EPR oximetry for pO_2 measurements in the beating rat hearts, *in vivo*.

The myocardial pO_2 measurements in the present study were performed using an *in vivo* EPR spectrometer (Magnettech, Berlin, Germany) equipped with automatic coupling and tuning controls for measurements in beating hearts. Microcrystals of LiNc-BuO were used as a probe for EPR oximetry. Rats, under inhalation anesthesia (air mixed with 1.5–2% isoflurane), were implanted with the oxygen-sensing probe in the left ventricular mid-myocardium. The animal was placed in a right lateral position with the chest open to the loop of a surface-coil resonator. EPR spectra were acquired as single 30-sec duration scans. The instrument settings were: microwave frequency, 1.2 GHz (L-band), incident microwave power, 4 mW; modulation amplitude, 180 mG, modulation frequency 100 kHz; receiver time constant, 0.2 sec. The peak-to-peak width of the EPR spectrum was used to calculate pO_2 using a standard calibration curve (47). Similarly, myocardial pO_2 was measured after 24 h of reperfusion.

Measurement of plasma nitrite/nitrate (NOx)

Plasma nitrite/nitrate (NOx) levels in the reperfused hearts were determined by Griess assay. The assay is based on the enzymatic conversion of nitrate to nitrite by nitrate reductase, followed by spectrophotometric quantitation (at 550 nm) of nitrite levels using the Griess reagent kit (Cayman Chemical, Ann Arbor, MI) and a Beckman AD 340 ELISA plate reader (Beckman Coulter, Fullerton, CA). Blood samples (0.5 ml) were collected at 1 h of reperfusion, centrifuged, and the plasma was stored at −80°C until analysis. The concentration of nitrite (indicative of NOx in the original samples) was calculated from a standard curve (1–35 μM) and used for determination of total nitrite/nitrate concentrations. The NOx levels were expressed as concentration (μM).

Histochemical staining of superoxide using DHE

Rats pretreated with vehicle-only (I/R), SPZ, L-NAME, SPZ + L-NAME were subjected to 30 min of LAD ligation, followed by 10 min reperfusion. Rats were sacrificed at 10 min of reperfusion and hearts were placed immediately in cold PBS and then embedded in optimal cutting temperature (OCT) compound for cryosectioning. Superoxide generation in the heart tissue was determined using hydroxyethidine (HE) fluorescence (42). The cell-permeable DHE is oxidized to fluorescent HE by superoxide, which is then intercalated into DNA. It has been reported (42) that the superoxide generation in hearts subjected to I/R occurs during the first 10 min of reperfusion. Hence, we measured the HE fluorescence at 10 min of reperfusion. The frozen segments from the heart tissue were cut into 6 μm thick sections that were then placed on glass slides. DHE (10 μM) was topically applied to each tissue section. The tissue sections on slides were incubated in a dark chamber at 37°C for 30 min and then washed three times

with PBS and fixed with aqueous mounting medium (Gel Mount, Sigma Chemicals). The images of the tissue sections were obtained using a fluorescence microscope (Nikon TE 300, Tokyo, Japan) with a rhodamine filter set (excitation = 550 nm; emission = 573 nm). Fluorescence intensity, which positively correlated with the levels of superoxide generation, was determined in the myocardial tissue using MetaMorph image analysis software (Molecular Devices).

Histochemical staining of NO using DAF-FM

The NO produced in I/R hearts was measured by fluorescence microscopy using DAF-FM diacetate. DAF-FM diacetate is cell permeable and passively diffuses across cellular membranes. Inside cells, DAF-FM diacetate is deacetylated by intracellular esterases to DAF-FM that reacts with NO to form fluorescent benzotriazole. Hearts, after 30 min of ischemia, and 10 min of reperfusion, were placed in an ice-cold PBS buffer and embedded in OCT compound for cryosectioning. The frozen tissues were cut into 6 μm thick sections and incubated with 10 μM DAF-FM diacetate for 30 min at 37°C. Images of the tissue sections were obtained using a fluorescence microscope (Nikon TE 300) with a fluorescein isothiocyanate (FITC) filter set (excitation = 495 nm; emission =510 nm). The fluorescence intensity, which positively correlated with the amount of NO generation, was quantitatively determined using MetaMorph image analysis software (Molecular Devices).

Immunohistochemical staining of iNOS

Immunostaining for iNOS was performed using formalin-fixed and paraffin-embedded heart tissue sections that were serially rehydrated in 100%, 95%, and 80% ethanol after deparaffinization with xylene. Slides were kept in a pre-heated steamer for 30 min for antigen retrieval, and then washed with PBS three times for 5 min each. Tissue sections were incubated with 2% goat serum and 5% bovine serum albumin in PBS to reduce nonspecific binding, followed by incubation with NOS2 (N-20) affinity-purified rabbit polyclonal antibody (1:100 dilution, Santa Cruz Biotechnology) for 1 h at room temperature in the humidity chamber. The sections were then incubated with secondary antibody (1:1,000 dilution) conjugated to green-fluorescent Alexa Fluor-488 dye. Separate tissue slides were stained without primary antibodies to examine nonspecific binding. The tissue sections were visualized using a Nikon fluorescence microscope equipped with an FITC filter set (excitation = 495 nm; emission = 510 nm) and the average intensity was calculated using MetaMorph image analysis software.

Immunohistochemical staining of nitrotyrosine

Paraformaldehyde-fixed and paraffin-embedded heart tissue sections were incubated with rabbit immuno-affinity-purified anti-nitrotyrosine antibody (at 1:100 dilution) for 1 h at room temperature in a humidity chamber. The sections were then incubated with biotinylated secondary antibody (biotinylated goat anti-rabbit antibody, ready-to-use, Lab Vision Corporation, Fremont, CA) for 1 h in the humidity chamber and streptavidin-horseradish peroxidase-conjugate solution for 30 min. Color was developed by using peroxidase diaminobenzidine substrate and counterstained with H&E stain. Negative controls were prepared by incubating the primary antibody with 10 mM nitrotyrosine in PBS for 1 h at room temperature, and using this solution instead of the primary antibody. For positive controls, rat hearts were infused with peroxynitrite (1 mM, 0.2 ml) into the LV chamber, and the hearts were removed and fixed in formalin/paraformaldehyde after 15 min of infusion. The slides were then processed and visualized using the above protocol.

Western blot analysis

Determination of iNOS protein was performed in samples taken from the area-at-risk of LV from I/R (control) and SPZ groups (3 rats in each group). Rats were anesthetized and sacrificed after 24 h of reperfusion. The hearts were rapidly explanted, rinsed in cold PBS (pH 7.4), containing 0.16 mg/ml heparin to remove red blood cells and clots, frozen in liquid nitrogen, and stored at −80°C. Tissue slices were taken from the area-at-risk (infarct region) of LV and were homogenized in buffer A (25 mM Tris HCl, pH 7.4, 0.5 mM EDTA, 0.5 mM EGTA, 1 mM phenylmethylsulfonyl fluoride, 1 mM dithiothreitol, 25 mM NaF, 1 mM Na_3VO_4, and 1% protease inhibitor (Sigma), and centrifuged at 10,000 g for 10 min at 4°C. The pellets were then incubated on ice in buffer B (buffer A plus 1% Triton X-100) for 2 h and centrifuged for 12 min at 4°C. The resulting supernatants were collected as membranous fractions. The expressions of NOS isoforms were assessed by standard SDS–PAGE Western immunoblotting techniques using polyclonal anti-iNOS (1:500 dilution) and monoclonal anti-β-actin antibodies. Similarly, phospho-specific antibodies (1:500 dilution) for Akt, ERK1/2, and p38 MAPK, followed by horseradish peroxidase-conjugated secondary antibodies (Amersham Biosciences, Piscataway, NJ) were used to determine the phosphorylation status of these proteins. The PVDF (polyvinylidene fluoride) membranes with transferred proteins were then developed by enhanced chemiluminescence. The same PVDF membranes were probed with antibodies for total Akt, ERK1/2, p38 MAPK, and β-actin. The protein intensities were quantified by an image-scanning densitometer (Scion Corporation, Frederick, MD). To quantify the phospho-specific signal in activated proteins, we first subtracted and then normalized the signal to the amount of actin or total target protein in the lysate (32). Data were expressed as percent of the expression in the control group.

Data analysis

The statistical significance of the results was evaluated using the one-way ANOVA and Student's t-test. The values were expressed as mean ± SD. A p value of <0.05 was considered significant.

Results

Myocardial tissue pO_2 in the ischemic/infarct region

I/R is associated with drastic changes in tissue oxygenation, which may have important implications in the early events leading to myocardial injury and dysfunction. In order to study the dynamics of tissue oxygenation during the I/R episode and to examine the effect of SPZ, we used *in vivo* EPR oximetry to monitor myocardial pO_2 in the infarct region continuously. We implanted an oxygen-sensing microcrystalline probe in the left ventricular mid-myocardium, in the region where ischemia would be expected to occur following

LAD ligation, and performed the pO_2 measurements under *in vivo* conditions (Fig. 1A–C). Figure 1D shows the changes in pO_2 during the 30 min ischemia followed by 60 min reperfusion in rats pretreated with SPZ + L-NAME, 1400W, and 1400W + SPZ. The basal (preischemic) levels of myocardial pO_2 were in the range of 18–20 mm Hg, and there were no significant differences among the groups. Immediately after induction of ischemia, the pO_2 levels dropped quickly and remained at ~2 mm Hg during the 30 min ischemic duration. Upon restoration of blood flow (reperfusion), a rapid increase in pO_2 leading to marked hyperoxygenation was observed in all groups. Further, the hyperoxygenation persisted for 60 min and beyond. Figure 1E shows the mean values of pO_2 obtained at the end of 60 min, as well as after 24 h reperfusion. At 60 min of reperfusion, the level of reoxygenation in untreated (I/R) hearts was significantly higher compared to non-I/R control (35 ± 2 *vs.* 19 ± 1 mm Hg). A similar hyperoxygenation was observed in all the treated groups. The SPZ group showed the maximum hyperoxygenation (45 ± 2 mm Hg), a more than twofold increase from the preischemic level. The hyperoxygenation was observed to be persistent and significant. However, the SPZ group showed a significant decrease in pO_2 at 24 h compared to 1 h, although the value was still substantially elevated in SPZ-treated hearts (38 ± 2 mm Hg) at 24 h. The hyperoxygenation in the SPZ group at 24 h was significantly attenuated compared to the I/R group

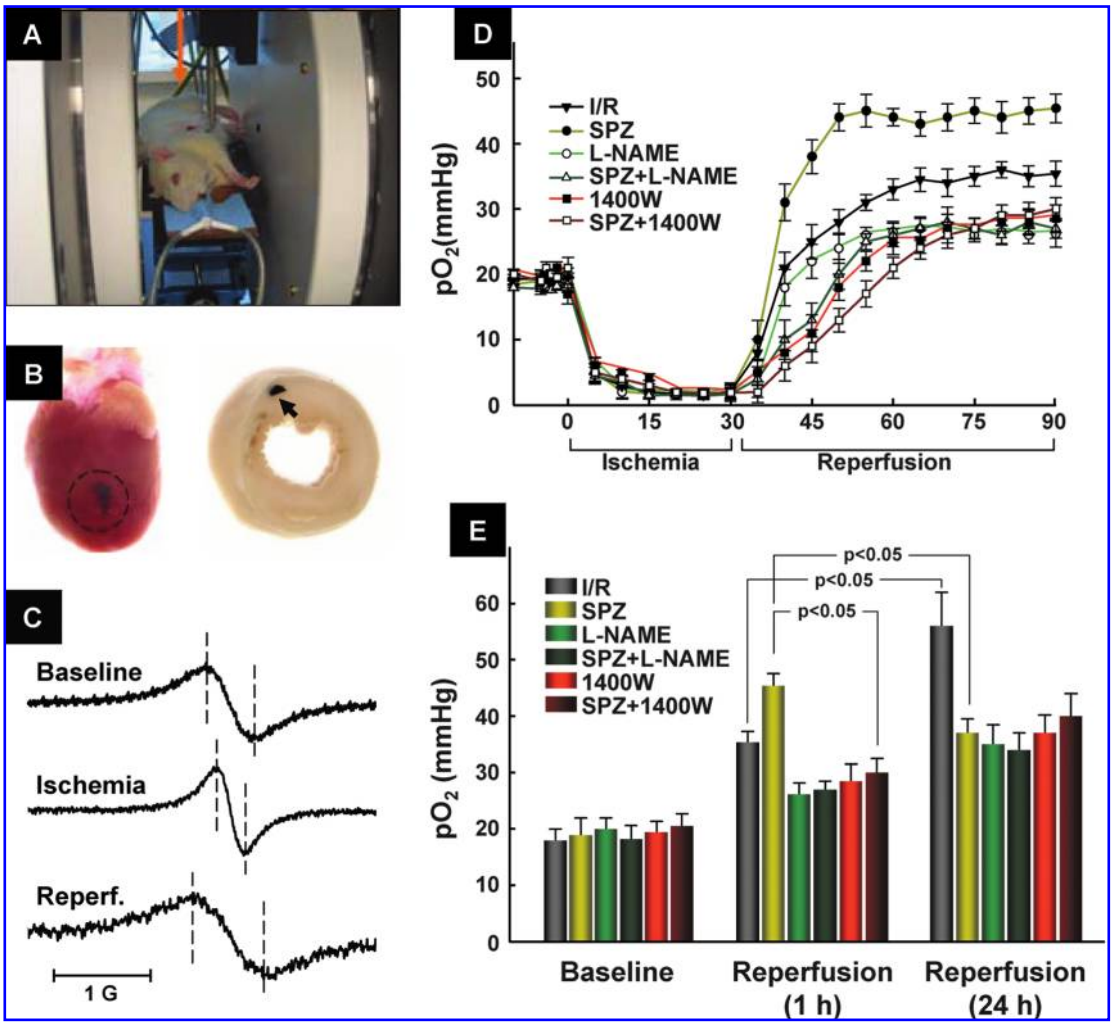

FIG. 1. ***In vivo*** **measurement of pO_2 in the rat heart using EPR oximetry**. (**A**) Placement of a rat in the EPR spectrometer for monitoring of myocardial oxygenation. The animal, under isoflurane inhalation anesthesia, is placed in a right lateral position with the chest open to the loop of a surface-coil resonator. (**B**) Implantation of oxygen-sensing microcrystals of LiNc-BuO in the left ventricular mid-myocardium. The probe particulates are seen as a black implant in the images of the whole heart and a formalin-fixed transverse slice through the left ventricle. The probe, which is nontoxic to tissue, responds to the partial pressure of oxygen (pO_2) at the site of placement. (**C**) Representative EPR signals obtained from a heart during preischemia (*baseline*), ischemia, and reperfusion. The peak-to-peak (*dashed line*) width of the signal is used to calculate pO_2 using a standard curve. (**D**) Changes in pO_2 during a 30 min ischemia, followed by 60 min reperfusion in rats pretreated with vehicle (I/R), SPZ, L-NAME, SPZ + L-NAME, 1400W, or SPZ + 1400W. Data represent mean ± SD, obtained from 6 animals/group. (**E**) Bar-graphical representation pO_2 data (mean ± SD, $n = 6$ animals/group) at the end of 1 h (from panel **D**) and at 24 h of reperfusion period. The "Baseline" data were obtained from preischemic hearts. The results show a significant oxygen overshoot (hyperoxygenation) during reperfusion. (For interpretation of the references to color in this figure legend, the reader is referred to the web version of this article at www.liebertonline.com/ars).

(56 ± 6 mm Hg). L-NAME or 1400W showed a similar increase in pO_2 up on reperfusion, however, the magnitude of hyperoxygenation was significantly less when compared to I/R or SPZ group at 1 h. The results further showed that co-administration of 1400W with SPZ significantly abrogated the hyperoxygenation observed in the SPZ group (30 ± 3 *vs.* 45 ± 2 mm Hg). The pO_2 data suggested that the hyperoxygenation observed in the SPZ group was possibly mediated through iNOS.

Heart rate and mean arterial blood pressure

Heart rate and mean arterial blood pressure were measured in rats before ischemia (baseline) and after 30 min ischemia and 1 h reperfusion (Fig. 2). There were no significant differences in the heart rates among I/R, SPZ, L-NAME, and SPZ + L-NAME groups during ischemia and reperfusion (Fig. 2). However, the mean arterial blood pressure was significantly reduced in all groups at the end of 30 min of ischemia. At 1 h reperfusion, the SPZ group showed a further significant drop in blood pressure when compared to the other groups.

Cardiac contractile function

Left ventricular contractile functions were measured after 24 h of reperfusion (Fig. 3). Rats pretreated with SPZ showed a significant improvement in LVSP, dP/dt_{max}, and dP/dt_{min} when compared to the I/R group. On the other hand, L-NAME or SPZ + L-NAME groups did not show any significant difference in the contractile functions when compared to the I/R group. Co-treatment of L-NAME and SPZ significantly blunted the recovery of contractility observed in the SPZ group.

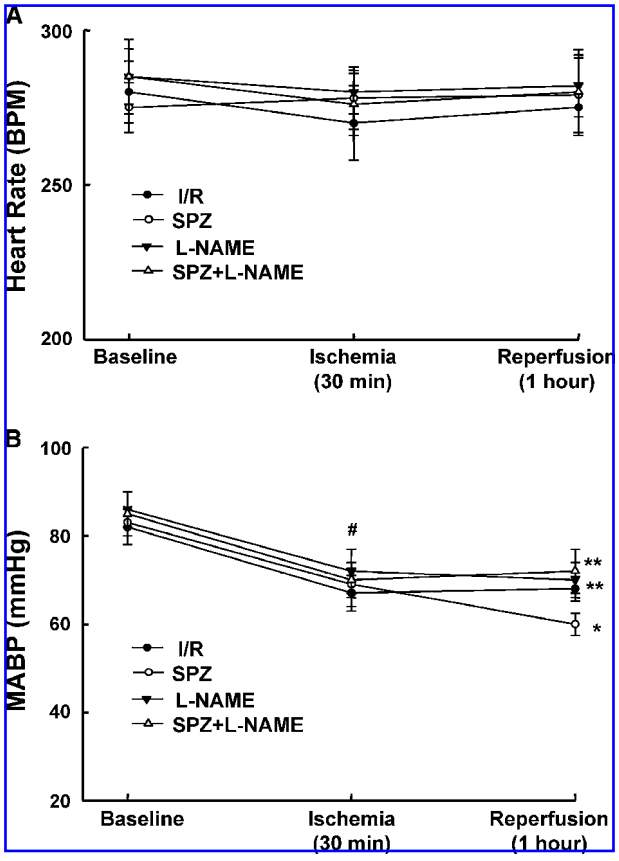

FIG. 2. Effect of SPZ on heart rate (HR) and mean arterial blood pressure (MABP) measured in carotid artery of rats. Hearts were subjected to 30 min ischemia, followed by 1 h reperfusion. Data represent mean ± SD ($n = 4$). $^{\#}p < 0.05$ *vs.* baseline, $^{*}p < 0.05$ *vs.* I/R group at 1 h reperfusion, $^{**}p < 0.05$ *vs.* SPZ group at 1 h reperfusion.

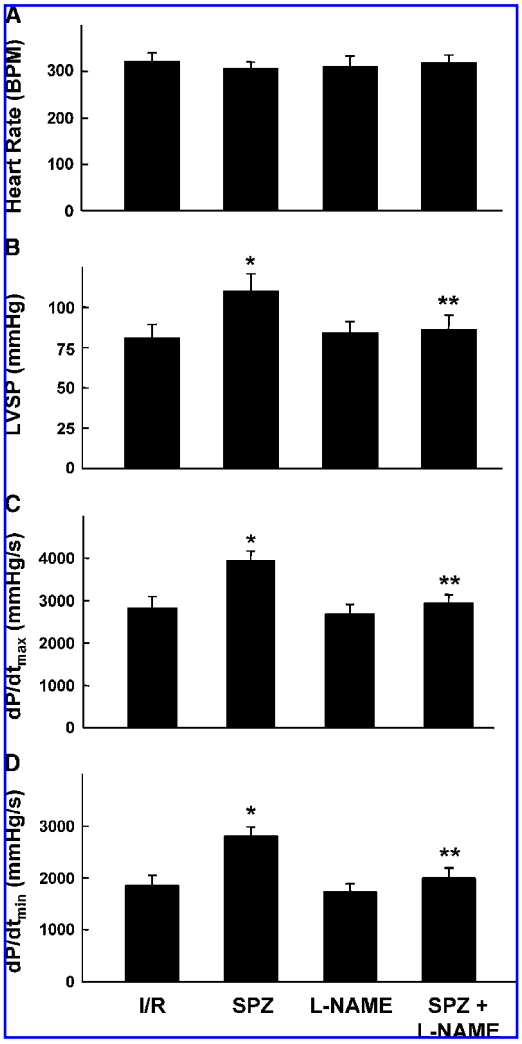

FIG. 3. Recovery of cardiac contractile functions. Rats, pretreated with SPZ and/or L-NAME, were subjected to 30 min of cardiac ischemia, followed by 24 h reperfusion. The following contractile parameters were measured using a Millar catheter inserted through the right carotid artery into LV: (**A**) heart rate, (**B**) left ventricular systolic pressure (LVSP), (**C**) maximum rate of increase of left ventricular pressure (dP/dt_{max}), and (**D**) maximum rate of decrease of left-ventricular pressure (dP/dt_{min}). Data represent mean ± SD ($n = 6$). $^{*}p < 0.05$ *vs.* I/R group; $^{**}p < 0.05$ *vs.* SPZ group. The results show a significant recovery of contractile function in the SPZ-treated group, while co-treatment of L-NAME with SPZ significantly blunted the beneficial effect observed in the SPZ group.

Myocardial infarct size

Myocardial infarct size was measured in rats subjected to 30 min of LAD ligation, followed by 24 h reperfusion (Fig. 4).

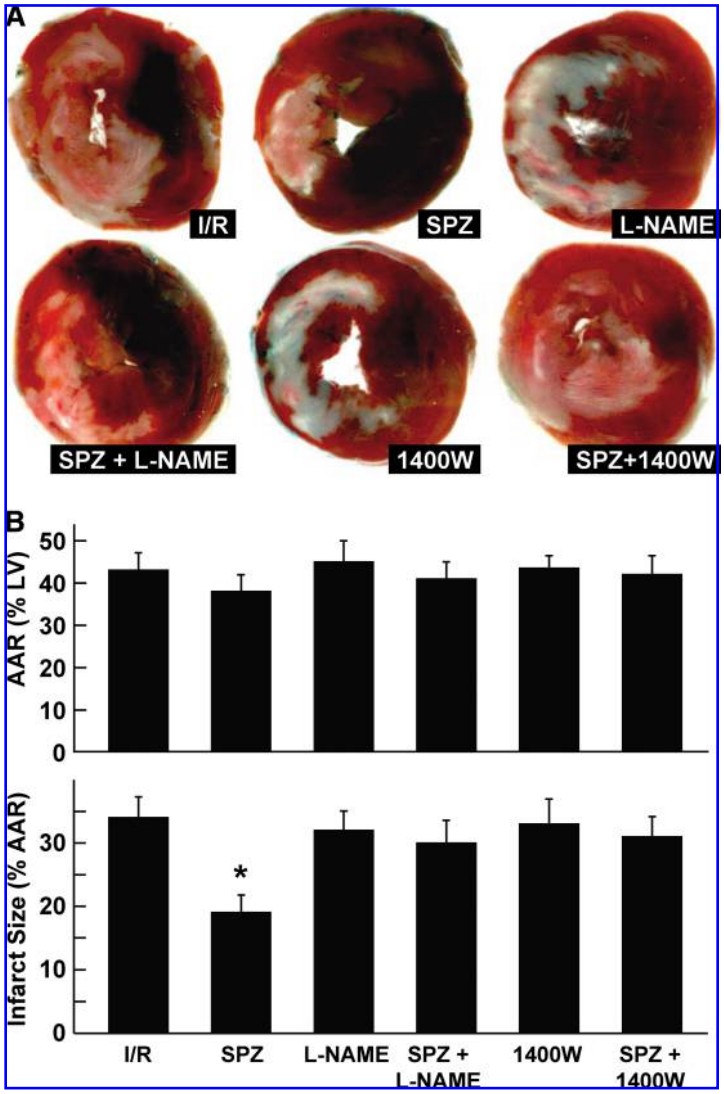

FIG. 4. Effect of SPZ pretreatment on myocardial infarct size. Images show triphenyltetrazolium chloride (TTC) sections of rat hearts pretreated with SPZ and/or L-NAME and subjected to 30 min ischemia, followed by 24 h reperfusion. Myocardial infarct size was measured using TTC staining. Evans blue and TTC staining were used to quantify the area-at-risk (*red*). The infarct region is shown by *white color*. (**A**) Representative sections of TTC-stained tissue are shown from I/R, SPZ, L-NAME, SPZ + L-NAME, 1400W, and SPZ + 1400W groups. (**B**) Infarct size. Data represent mean ± SD ($n = 6$). *$p < 0.05$ *vs.* I/R group. The infarct size was significantly decreased in rats pretreated with SPZ compared to I/R, L-NAME, SPZ + L-NAME, 1400W, and SPZ + 1400W groups. (For interpretation of the references to color in this figure legend, the reader is referred to the web version of this article at www.liebertonline.com/ars).

The infarct area, expressed as percent of area-at-risk (AAR), was significantly less in rats pretreated with SPZ compared to untreated (I/R) rats (19 ± 2.5% *vs.* 34 ± 3.3%). There was no significant difference in the infarct size in groups pretreated with L-NAME (32 ± 3.1%), SPZ + L-NAME (30 ± 3.6%), 1400W (33 ± 4%) or SPZ + 1400W (31 ± 3.2%) when compared to the I/R group. Combined treatment of 1400W or L-NAME with SPZ significantly blunted the beneficial effect of SPZ.

Plasma levels of nitrite/nitrate (NOx)

To determine the effect of SPZ on the NO levels, the plasma levels of stable metabolites of NO, namely, nitrite and nitrate (NOx) were determined after 1-h reperfusion (Fig. 5). Control hearts subjected to I/R showed a significantly increased plasma NOx level compared to non-I/R hearts. On the other hand, SPZ-treated hearts showed a further significant increase in NOx levels when compared to the I/R group. L-NAME and SPZ + L-NAME treatments significantly attenuated the plasma NOx levels, suggesting that the increase in NOx levels in

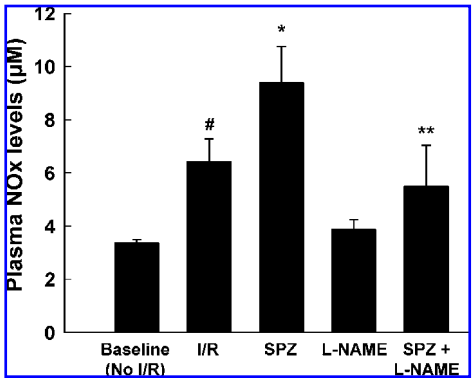

FIG. 5. Effect of SPZ on plasma nitrite/nitrate (NOx) levels. Rats, pretreated with SPZ and/or L-NAME, were subjected to 30 min of cardiac ischemia, followed by reperfusion. Blood samples were collected from Baseline (no I/R), I/R, SPZ, L-NAME, and SPZ + L-NAME groups at 1 h of reperfusion. Data represent mean ± SD ($n = 4$). #$p < 0.05$ *vs.* Baseline group; *$p < 0.05$ *vs.* I/R group; **$p < 0.05$ *vs.* SPZ group.

the SPZ-treated group was derived from an L-NAME inhibitable source.

Effect of SPZ on superoxide, NO, and peroxynitrite

Superoxide, NO, peroxynitrite, and iNOS levels in the infarct tissue sections of hearts subjected to 30 min LAD occlusion, followed by 10 min or 24 h reperfusion, were measured by histochemical staining and fluorescence microscopy (Fig. 6). The level of superoxide at 10 min reperfusion was significantly elevated in the I/R group. The SPZ-treated group showed a significant reduction in superoxide generation when compared to the I/R group. Administration of L-NAME, either alone or in combination with SPZ, did not have

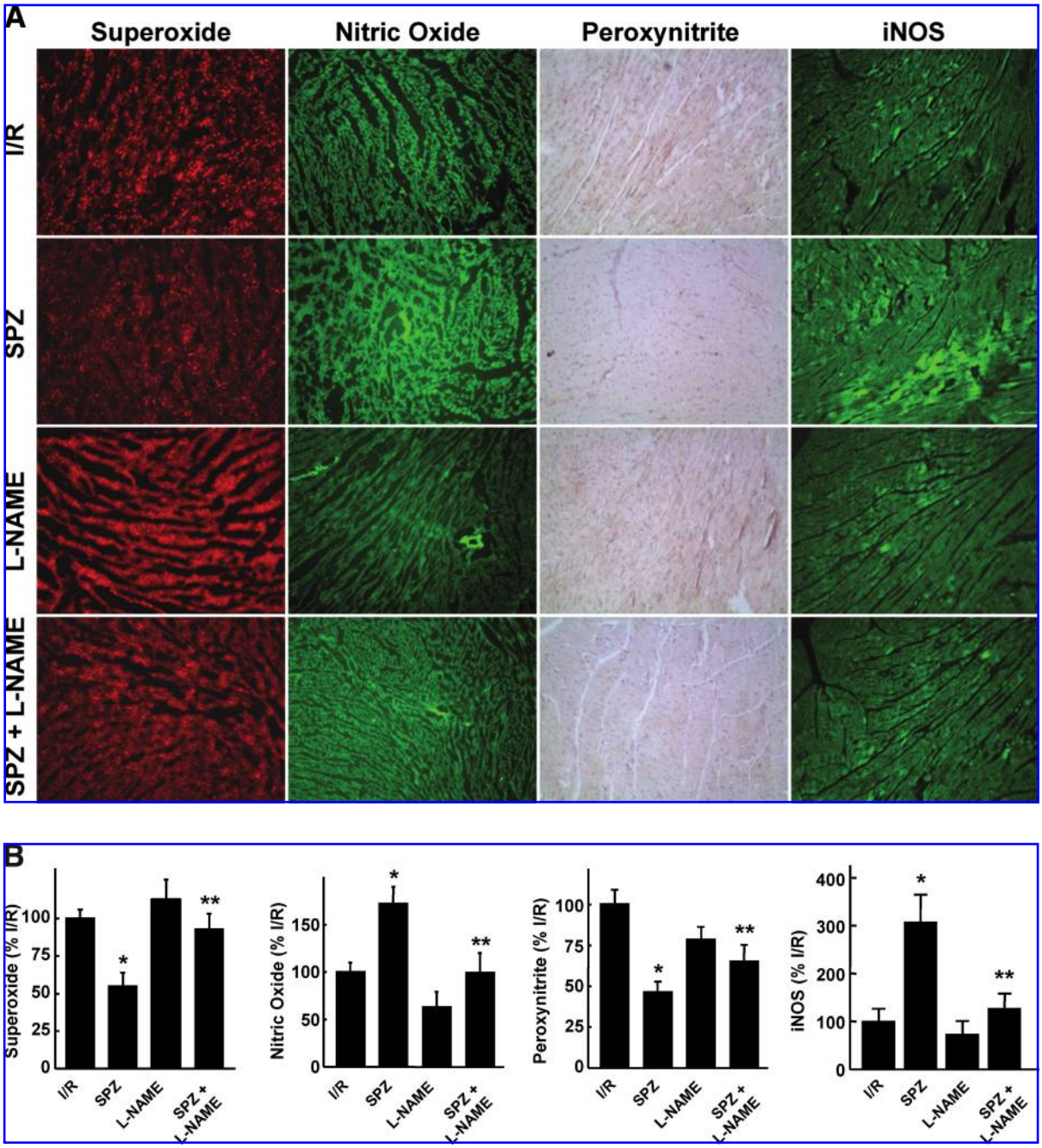

FIG. 6. Effect of SPZ on the tissue levels of superoxide, nitric oxide, peroxynitrite, and iNOS in the infarct heart. Superoxide and nitric oxide levels in the excised heart tissue were determined by histochemical staining and fluorescence microscopy at 10 min of reperfusion. Peroxynitrite and iNOS levels in the excised heart tissue were determined by immunohistochemical staining and fluorescence microscopy at 24 h of reperfusion. (**A**) Representative images (at 200x magnification) of superoxide, nitric oxide, peroxynitrite, and iNOS from tissue sections obtained from hearts treated with SPZ ± L-NAME. (**B**) Mean fluorescence intensity from triplicate hearts. Data represent mean ± SD. *$p < 0.05$ *vs.* I/R group; **$p < 0.05$ *vs.* SPZ group. (For interpretation of the references to color in this figure legend, the reader is referred to the web version of this article at www.libertonline.com/ars).

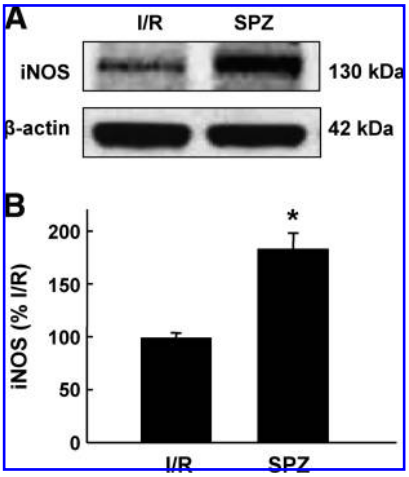

FIG. 7. Western blot analysis of iNOS expression in hearts treated with SPZ. Rat hearts were subjected to 30 min ischemia, followed by 24 h reperfusion. (**A**) Representative immunoblots of iNOS expression and β-actin in I/R and SPZ-treated hearts. (**B**) Densitometric analysis of iNOS expression. Results are expressed as mean ± SD of three hearts in each group; $*p < 0.05$ *vs.* I/R group.

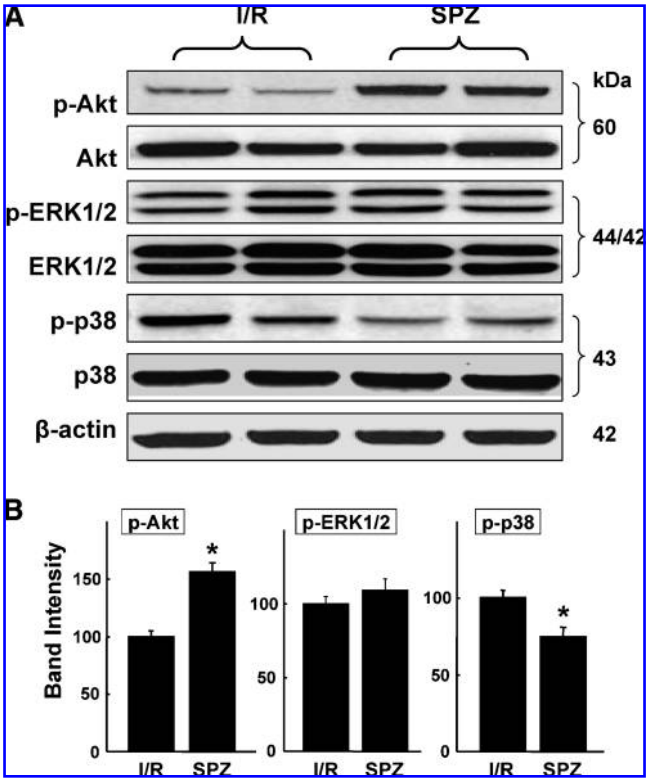

FIG. 8. Effect of SPZ on the I/R-induced phosphorylation of key signaling proteins. The levels of total and activated levels of Akt, ERK1/2, and p38 MAPK were measured in hearts subjected to 30 min of ischemia, followed by 24-h reperfusion. (**A**) Representative Western blots of total and phosphorylated Akt, ERK1/2, and p38 MAPK. (**B**) Quantitative analysis (band intensity) of phosphorylated Akt, ERK1/2, and p38 MAPK. Results are expressed as mean ± SD ($n = 3$ hearts) from each group. $*p < 0.05$ *vs.* I/R group.

any significant effect on superoxide generation upon reperfusion. The results clearly indicated that SPZ attenuated the formation of superoxide radicals during the early phase of reperfusion. The NO level in the hearts at 10 min of reperfusion was significantly higher in SPZ-treated hearts, when compared to the I/R group (Fig. 6). However, in L-NAME and SPZ + L-NAME groups, there was a significant decrease of NO as compared to the SPZ group. The results suggested that SPZ enhanced myocardial tissue NO bioavailability during the early phase of reperfusion.

Peroxynitrite ($OONO^-$), a potent oxidant formed by the reaction of superoxide with NO, has been implicated in I/R injury (52). In order to determine whether SPZ could attenuate peroxynitrite generation in the reperfused heart, we used nitrotyrosine-staining to quantify the myocardial tissue levels of peroxynitrite. Untreated rats subjected to 24 h reperfusion exhibited a substantially high level of peroxynitrite (Fig. 6). Pretreatment of rats with SPZ showed a significant reduction of peroxynitrite formation. On the other hand, rats pretreated with L-NAME alone or L-NAME + SPZ did not show any significant difference in the peroxynitrite levels when compared to the I/R group.

Effect of SPZ on iNOS expression

SPZ has been shown to increase the bioavailability of NO by decreasing superoxide generation in the reperfused heart (23, 31). However, its effect on the induction of NO-generating enzymes such as iNOS in the heart upon reperfusion is not known. We measured the level of iNOS protein in the tissue sections of rat hearts subjected to 24 h reperfusion (Fig. 6). The iNOS level was significantly increased (threefold) in the SPZ-treated hearts when compared to the untreated (I/R) group. Rats pretreated with L-NAME alone or L-NAME with SPZ did not show any significant difference in the iNOS levels when compared to the untreated I/R group. The upregulation of iNOS by SPZ was further confirmed by Western blot analysis. There was a significant increase of iNOS expression in the SPZ group when compared to I/R control (Fig. 7).

Effect of SPZ on phosphorylation of Akt, ERK1/2 and p38 MAPK

To further understand the underlying mechanism of signaling pathways leading to the attenuation of post-ischemic reperfusion injury in the hearts treated with SPZ, we performed SDS-PAGE and Western blot assays for phosphorylated Akt, ERK1/2, and p38 MAPK in the rat heart homogenates. The SPZ group showed a significant increase in the phosphorylation of Akt when compared to the I/R group (Fig. 8). However, there was no significant change in the phosphorylation of ERK1/2 in the SPZ and I/R groups. In contrast, there was a significant increase in p38 MAPK in the I/R group when compared to the SPZ group. SPZ treatment markedly ameliorated I/R-induced activation of p38 MAPK compared to the I/R group. Overall, the Western blot analyses indicated that SPZ treatment enhanced the activation of Akt and attenuated the phosphorylation of p38 MAPK, thereby

conferring cardioprotection. However, the results do not confirm a direct effect of SPZ on these proteins.

Discussion

The present study showed that pretreatment of rats with SPZ significantly diminished the myocardial damage and dysfunction caused by reperfusion. The beneficial effects correlated with a significant elevation of tissue oxygenation and bioavailability of NO. Reperfusion of ischemic myocardium is known to compromise the bioavailability of NO, which is mainly attributed to impairment of key enzymes and substrates responsible for its production (41, 68). In addition, the loss of NO bioavailability could also occur as a result of inactivation of NO by superoxide radicals that are known to be abundantly generated in the reperfused myocardium (69). The present results suggest that the augmentation of NO bioavailability by SPZ is mainly due to overexpression of iNOS enzyme. The results further suggest that the superoxide-scavenging ability of SPZ may also be responsible for the enhanced bioavailability of NO and decreased levels of peroxynitrite in the reperfused myocardium. The involvement of NO in cardioprotection is obvious from the observation that addition of L-NAME or 1400W attenuated both NO levels and the cardioprotective capacity of SPZ. Most importantly, the large increase in myocardial tissue oxygenation observed in the SPZ group could be due to NO bioavailability, leading to increased myocardial blood flow at reperfusion.

The superoxide, peroxynitrite, and NO levels at 10 min of reperfusion (Fig. 6) suggest that the cardioprotective effect of SPZ may be due to any one, or a combination of the following factors: (a) inhibition/scavenging of superoxide radicals; (b) increased bioavailability of NO upon reperfusion; (c) decreased systemic vascular resistance and/or aortic input impedance (most importantly, coronary vascular) resistance; and (d) improved myocardial energetics. The myocardial energetics refer to the balance between myocardial oxygen delivery and consumption.

In the present study, the baseline (preischemic) myocardial tissue oxygenation did not change among the four groups. However, there was a substantial hyperoxygenation in all groups upon reperfusion. The hyperoxygenation in the SPZ group at 1 h reperfusion was significantly higher when compared to the untreated, L-NAME, or 1400W group. The increase in pO_2 at 1 h reperfusion in the SPZ group could be attributed to the enhanced NO levels, which may cause increased blood flow upon reperfusion. The marked hyperoxygenation could also occur as a result of decreased oxygen consumption due to NO-mediated inhibition of mitochondrial respiration (67). On the other hand, the differences in the levels of myocardial oxygenation among the groups at 24 h reperfusion could reflect the decrease in oxygen demand as a result of varying levels of infarction. It should be noted that only in the case of the SPZ group did we observe a decrease in the oxygenation at 24 h compared to 1 h into reperfusion, which is reflective of the substantial reduction in the infarct size found within the SPZ group. Overall, the magnitude and temporal changes in myocardial tissue oxygenation apparently reflects the physiological and metabolic alterations due to acute changes in the tissue levels of nitric oxide, oxidants, and oxygen consumption.

The three prime determinants of oxygen consumption are heart rate, contractility, and peak myocardial tension (afterload). Heart rate was unchanged by SPZ, but the increase in dP/dt_{max} and peak systolic pressure would be expected to increase oxygen demand and to decrease myocardial oxygen content. However, we observed an increase in the myocardial oxygen content upon reperfusion of SPZ-treated hearts. There are two possible explanations as to why myocardial oxygen content was increased by SPZ. One possibility is that the preload end-diastolic radius of the LV chamber could be reduced, the LV wall would thicken, and both decreased radius and increased wall-thickness would lead to a decrease in afterload despite elevation of systolic pressure. Second, the decrease in coronary vascular resistance (caused by NO) might have been out of proportion to the effect on the general systemic arterial resistance of vessels. Thus, the decrease in preload and afterload, along with the increased coronary flow, would result in the observed increase in myocardial oxygen content.

The increase in peak systolic pressure in the SPZ-treated hearts (Fig. 3B) may be attributed to increased stroke volume, stiffening of the aorta (increasing elasticity modulus), or increased systemic vascular resistance. However, the depressed systemic arterial blood pressure (Fig. 2B) might indicate a decrease in the systemic arterial diastolic pressure, which is the determinant of afterload and myocardial oxygen consumption. The decrease in systemic arterial pressure and the increase in stroke volume are consistent with the known pharmacology of NO (29).

Among the inhibitors of nitric oxide synthases, 1400W is by far the most selective for inhibiting the activity of iNOS. Its ratio of selectivity for iNOS *versus* eNOS is >4,000-fold, which is in sharp contrast to that of aminoguanidine (11-fold), N5-iminoethyl-L-ornithine (49-fold) (1) or isothiourea (2–6 fold) (21). In addition, the *in vitro* potency of 1400W in inhibiting iNOS is 135- and 19-times that of aminoguanidine and N5-iminoethyl-L-ornithine, respectively (1). Studies have shown that 1400W is effective in reversing vascular abnormalities known to be associated with the induction of iNOS (21, 53, 58). The widely accepted mechanism of action of 1400W is its inhibitory effect on iNOS activity.

Studies have shown that ROS produced in the myocardium at the onset of reperfusion can cause tissue and functional injury, which is preventable, at least in part, by antioxidants (2, 32–34, 51, 56). Peroxynitrite ($ONOO^-$), a dominant reaction product of NO and superoxide (16), has been reported to increase apoptosis in a variety of cell types. The proapoptotic mechanisms of $ONOO^-$ include protein and DNA oxidation (10), lipid peroxidation (60), protein nitration (19, 22, 40), apoptosis-inducing factor release (66), and endoplasmic reticulum stress, with the subsequent release of caspase (46). Our results showed that pretreatment with SPZ markedly reduced cardiac nitrotyrosine content, indicating that SPZ blocks nitrative stress through inhibition of peroxynitrite formation. The decrease in peroxynitrite in the SPZ-treated rat hearts could be due to attenuation of superoxide radicals by SPZ, thereby limiting the reaction of superoxide with NO (31).

The iNOS-dependent biosynthesis of NO is a common pathway involved in the protection of heart against various forms of stress (6, 7). Ischemic preconditioning (IPC) has been

shown to upregulate iNOS expression in cardiac myocytes (27, 62). A relatively modest upregulation of iNOS, such as that known to occur during late preconditioning, is cardioprotective, whereas a massive upregulation of iNOS that may occur during inflammation or septic shock could be detrimental (24, 62). Enhanced expression of iNOS and NO production has been implicated in the cardioprotection by several drugs including resveratrol (27, 62), sildenafil (53), and atorvastatin (3). The results of the present study clearly indicated an upregulation of iNOS expression by SPZ, suggesting that NO derived from iNOS was responsible for the cardioprotection in the SPZ-treated hearts.

Activation of Akt and ERK1/2 has been shown to be cardioprotective (38, 59). In the heart, the p38 MAPK pathway has been implicated in the regulation of cardiac gene expression, myocyte hypertrophy, inflammation, bioenergetics, contractility and proliferation, and apoptosis (4, 15, 49). Studies have also shown that activation of p38 MAPK enhances lethal injury and inhibition of p38 MAPK by SB203580 (MAPK inhibitor) reduces postischemic myocardial apoptosis (39). Several proapoptotic proteins have been identified as direct Akt substrates, including Bad, caspase-9, and apoptosis-signal regulating kinase (ASK1). Phosphorylation of these molecules by Akt may reduce apoptotic cell death by inhibiting caspase-9 activity, releasing antiapototic molecule Bcl-2, blocking proapoptotic molecules Fas ligand expression, and inhibiting proapoptotic p38 MAPK activation (11, 20). In the present study, we observed that SPZ activated Akt and decreased the activity of p38 MAPK, which might lead to a decrease in myocyte apoptosis and thereby protecting the heart against I/R injury. However, the exact mechanisms by which SPZ mediates enhancement of Akt and inhibition of p38 MAPK activities are yet to be elucidated.

Wang *et al.* (61) have demonstrated that Akt phosphorylation by diazoxide is upstream of NOS, and NOS and Akt phosphorylation are important in preventing cell death in the ischemic myocardium. Diazoxide was shown to be an important agonist of mitoKATP channel opener and exert its antiapoptotic effect through the PI3 kinase-Akt pathway. Further, the phosphorylation of eNOS with subsequent NO production is an important downstream effector that contributes significantly to the cardioprotective effect of diazoxide against I/R injury. Similarly, in our study we have observed that SPZ activated Akt expression and decreased the expression of p38 MAPK, which might lead to decrease in myocyte apoptosis and thereby protecting the heart against I/R injury. However, the exact mechanism by which SPZ mediates enhancement of Akt and inhibition of p38 MAPK activity is yet to be understood.

The pO_2 measurements were performed by EPR oximetry using an oxygen-sensing paramagnetic microcrystalline probe (47). The probe is nontoxic and stable in tissues without undergoing phagocytosis by macrophages or clearance from the site of implant. The probe is also stable against biological oxido-reductants including superoxide, nitric oxide, hydrogen peroxide, ascorbate, or glutathione. Both the EPR-detection sensitivity (paramagnetism) and oxygen-sensitivity calibration (line-broadening by oxygen) are stable for long periods, thus, enabling repeated measurements. Finally, the probe reports absolute values of pO_2 in the microenvironment at the site of implantation. Since multiple crystals are used, the measured value is an average of readings from the entire implant, which is usually a point deposit, as seen in Fig. 1B.

To our knowledge, this is the first report of *in situ* oxygenation measurements in the beating heart of a live rat. The EPR oximetry in the heart requires one-time surgical implantation of the oxygen-sensing microcrystals at the site of interest. Subsequent measurements can be performed noninvasively and precisely at the site of implantation for extended periods of time, possibly weeks or months, without having to open the chest or reintroduce the probe (30). At present, these measurements are only limited to the hearts of closed-chest rodents such as mice and small rats. In larger-sized rats, such as that used in the present study, it is necessary to make an incision in the chest to allow the resonator (pick-up coil) access to the region of interest to obtain a detectable EPR signal. Nevertheless, the measurements reported in this work were done on open-chest rats during the 90 min period, and then on reopened chests after 24 h. Despite the technical challenges and limitations, very precise and reliable oxygen measurements from the beating heart could be obtained using EPR oximetry.

In summary, pretreatment of rats with SPZ ameliorated I/R-induced myocardial damage and improved cardiac contractile functions by decreasing superoxide production, peroxynitrite formation, and by enhancing NO bioavailability, myocardial tissue oxygenation, and iNOS expression. SPZ treatment also activated pro-survival Akt, leading to the attenuation of proapoptotic p38 MAPK. Overall, this study established that SPZ induces iNOS expression and modulates important signaling pathways involved in cardioprotection.

Acknowledgments

This work was supported by National Institutes of Health Grant EB006153.

Abbreviations

AAR, area at risk; CYP, cytochrome P450; DAF-FM, 4-amino-5-methylamino-2′,7′-difluorofluorescein; DHE, dihydroethidium; EPR, electron paramagnetic resonance; HE, hydroxyethidine; I/R, ischemia/reperfusion; iNOS, inducible nitric oxide synthase; IPC, ischemic preconditioning; LAD, left anterior descending coronary artery; LiNc-BuO, lithium octa-n-butoxynaphthalocyanine; L-NAME, N^{ω}-nitro-L-arginine methylester; LVSP, left ventricular systolic pressure; MI, myocardial infarction; NO, nitric oxide; NOS, nitric oxide synthase; $OONO^{-}$, peroxynitrite; ROS, reactive oxygen species; SPZ, sulfaphenazole; TTC, 2,3,5-triphenyltetrazolium chloride.

Disclosure Statement

No competing financial interests exist.

References

1. Alderton WK, Cooper CE, and Knowles RG. Nitric oxide synthases: structure, function and inhibition. *Biochem J* 357: 593–615, 2001.
2. Ambrosio G, Zweier JL, and Flaherty JT. The relationship between oxygen radical generation and impairment of

myocardial energy metabolism following post-ischemic reperfusion. *J Mol Cell Cardiol* 23: 1359–1374, 1991.
3. Atar S, Ye Y, Lin Y, Freeberg S Y, Nishi SP, Rosanio S, Huang MH, Uretsky BF, Perez–Polo JR, and Birnbaum Y. Atorvastatin-induced cardioprotection is mediated by increasing inducible nitric oxide synthase and consequent S-nitrosylation of cyclooxygenase-2. *Am J Physiol Heart Circ Physiol* 290: H1960–1968, 2006.
4. Baines CP and Molkentin JD. STRESS signaling pathways that modulate cardiac myocyte apoptosis. *J Mol Cell Cardiol* 38: 47–62, 2005.
5. Bhuiyan MS and Fukunaga K. Inhibition of HtrA2/Omi ameliorates heart dysfunction following ischemia/reperfusion injury in rat heart *in vivo*. *Eur J Pharmacol* 557: 168–177, 2007.
6. Bolli R. The late phase of preconditioning. *Circ Res* 87: 972–983, 2000.
7. Bolli R, Dawn B, Tang XL, Qiu Y, Ping P, Xuan YT, Jones WK, Takano H, Guo Y, and Zhang J. The nitric oxide hypothesis of late preconditioning. *Basic Res Cardiol* 93: 325–338, 1998.
8. Chen Z, Oberley TD, Ho Y, Chua CC, Siu B, Hamdy RC, Epstein CJ, and Chua BH. Overexpression of CuZnSOD in coronary vascular cells attenuates myocardial ischemia/reperfusion injury. *Free Radic Biol Med* 29: 589–596, 2000.
9. Chen Z, Siu B, Ho YS, Vincent R, Chua CC, Hamdy RC, and Chua BH. Overexpression of MnSOD protects against myocardial ischemia/reperfusion injury in transgenic mice. *J Mol Cell Cardiol* 30: 2281–2289, 1998.
10. Chiarugi A and Moskowitz MA. Cell biology. PARP-1—a perpetrator of apoptotic cell death? *Science* 297: 200–201, 2002.
11. Cross TG, Scheel–Toellner D, Henriquez NV, Deacon E, Salmon M, and Lord JM. Serine/threonine protein kinases and apoptosis. *Exp Cell Res* 256: 34–41, 2000.
12. Das DK and Maulik N. Antioxidant effectiveness in ischemia-reperfusion tissue injury. *Methods Enzymol* 233: 601–610, 1994.
13. Depre C, Fierain L, and Hue L. Activation of nitric oxide synthase by ischaemia in the perfused heart. *Cardiovasc Res* 33: 82–87, 1997.
14. Elmi S, Sallam NA, Rahman MM, Teng X, Hunter L, Moien–Afshari F, Khazaei M, Granville DJ, and Laher I. Sulfaphenazole treatment restores endothelium-dependent vasodilation in diabetic mice. *Vascul Pharmacol* 48: 1–8, 2008.
15. Engel FB. Cardiomyocyte proliferation: A platform for mammalian cardiac repair. *Cell Cycle* 4: 1360–1363, 2005.
16. Ferdinandy P. Peroxynitrite: Just an oxidative/nitrosative stressor or a physiological regulator as well? *Br J Pharmacol* 148: 1–03, 2006.
17. Fichtlscherer S, Dimmeler S, Breuer S, Busse R, Zeiher AM, and Fleming I. Inhibition of cytochrome P450 2C9 improves endothelium-dependent, nitric oxide-mediated vasodilatation in patients with coronary artery disease. *Circulation* 109: 178–0183, 2004.
18. Fleming I, Michaelis UR, Bredenkotter D, Fisslthaler B, Dehghani F, Brandes RP, and Busse R. Endothelium-derived hyperpolarizing factor synthase (Cytochrome P450 2C9) is a functionally significant source of reactive oxygen species in coronary arteries. *Circ Res* 88: 44–051, 2001.
19. Francescutti D, Baldwin J, Lee L, and Mutus B. Peroxynitrite modification of glutathione reductase: modeling studies and kinetic evidence suggest the modification of tyrosines at the glutathione disulfide binding site. *Protein Eng* 9: 189–194, 1996.
20. Gao F, Gao E, Yue TL, Ohlstein EH, Lopez BL, Christopher TA, and Ma XL. Nitric oxide mediates the antiapoptotic effect of insulin in myocardial ischemia-reperfusion: the roles of PI3-kinase, Akt, and endothelial nitric oxide synthase phosphorylation. *Circulation* 105: 1497–1502, 2002.
21. Garvey EP, Oplinger JA, Furfine ES, Kiff RJ, Laszlo F, Whittle BJ, and Knowles RG. 1400W is a slow, tight binding, and highly selective inhibitor of inducible nitric-oxide synthase *in vitro* and *in vivo*. *J Biol Chem* 272: 4959–4963, 1997.
22. Gow AJ, Duran D, Malcolm S, and Ischiropoulos H. Effects of peroxynitrite-induced protein modifications on tyrosine phosphorylation and degradation. *FEBS Lett* 385: 63–66, 1996.
23. Granville DJ, Tashakkor B, Takeuchi C, Gustafsson AB, Huang C, Sayen MR, Wentworth P, Jr., Yeager M, and Gottlieb RA. Reduction of ischemia and reperfusion-induced myocardial damage by cytochrome P450 inhibitors. *Proc Natl Acad Sci USA* 101: 1321–1326, 2004.
24. Guo Y, Jones WK, Xuan YT, Tang XL, Bao W, Wu WJ, Han H, Laubach VE, Ping P, Yang Z, Qiu Y, and Bolli R. The late phase of ischemic preconditioning is abrogated by targeted disruption of the inducible NO synthase gene. *Proc Natl Acad Sci USA* 96: 11507–11512, 1999.
25. Hearse DJ and Bolli R. Reperfusion induced injury: manifestations, mechanisms, and clinical relevance. *Cardiovasc Res* 26: 101–108, 1992.
26. Hunter AL, Cruz RP, Cheyne BM, McManus BM, and Granville DJ. Cytochrome p450 enzymes and cardiovascular disease. *Can J Physiol Pharmacol* 82: 1053–1060, 2004.
27. Imamura G, Bertelli AA, Bertelli A, Otani H, Maulik N, and Das DK. Pharmacological preconditioning with resveratrol: an insight with iNOS knockout mice. *Am J Physiol Heart Circ Physiol* 282: H1996–2003, 2002.
28. Jones SP, Greer JJ, Kakkar AK, Ware PD, Turnage RH, Hicks M, van Haperen R, de Crom R, Kawashima S, Yokoyama M, and Lefer DJ. Endothelial nitric oxide synthase overexpression attenuates myocardial reperfusion injury. *Am J Physiol Heart Circ Physiol* 286: H276–282, 2004.
29. Kelly RA, Balligand JL, and Smith TW. Nitric oxide and cardiac function. *Circ Res* 79: 363–380, 1996.
30. Khan M, Kutala VK, Vikram DS, Wisel S, Chacko SM, Kuppusamy ML, Mohan IK, Zweier JL, Kwiatkowski P, and Kuppusamy P. Skeletal myoblasts transplanted in the ischemic myocardium enhance in situ oxygenation and recovery of contractile function. *Am J Physiol Heart Circ Physiol* 293: H2129–2139, 2007.
31. Khan M, Mohan IK, Kutala VK, Kumbala D, and Kuppusamy P. Cardioprotection by sulfaphenazole, a cytochrome p450 inhibitor: mitigation of ischemia-reperfusion injury by scavenging of reactive oxygen species. *J Pharmacol Exp Ther* 323: 813–821, 2007.
32. Khan M, Varadharaj S, Ganesan LP, Shobha JC, Naidu MU, Parinandi NL, Tridandapani S, Kutala VK, and Kuppusamy P. C-phycocyanin protects against ischemia-reperfusion injury of heart through involvement of p38 MAPK and ERK signaling. *Am J Physiol Heart Circ Physiol* 290: H2136–2145, 2006.
33. Kutala VK, Khan M, Angelos MG, and Kuppusamy P. Role of oxygen in postischemic myocardial injury. *Antioxid Redox Signal* 9: 1193–1206, 2007.
34. Kutala VK, Khan M, Mandal R, Potaraju V, Colantuono G, Kumbala D, and Kuppusamy P. Prevention of postischemic myocardial reperfusion injury by the combined treatment of NCX-4016 and Tempol. *J Cardiovasc Pharmacol* 48: 79–87, 2006.

35. Kutala VK, Parinandi NL, Pandian RP, and Kuppusamy P. Simultaneous measurement of oxygenation in intracellular and extracellular compartments of lung microvascular endothelial cells. *Antioxid Redox Signal* 6: 597–603, 2004.
36. Lefer AM. Attenuation of myocardial ischemia-reperfusion injury with nitric oxide replacement therapy. *Ann Thorac Surg* 60: 847–851, 1995.
37. Liaudet L, Soriano FG, and Szabo C. Biology of nitric oxide signaling. *Crit Care Med* 28: N37–52, 2000.
38. Liu HR, Gao F, Tao L, Yan WL, Gao E, Christopher TA, Lopez BL, Hu A, and Ma XL. Antiapoptotic mechanisms of benidipine in the ischemic/reperfused heart. *Br J Pharmacol* 142: 627–634, 2004.
39. Ma XL, Kumar S, Gao F, Louden CS, Lopez BL, Christopher TA, Wang C, Lee JC, Feuerstein GZ, and Yue TL. Inhibition of p38 mitogen-activated protein kinase decreases cardiomyocyte apoptosis and improves cardiac function after myocardial ischemia and reperfusion. *Circulation* 99: 1685–1691, 1999.
40. MacMillan–Crow LA, Crow JP, and Thompson JA. Peroxynitrite-mediated inactivation of manganese superoxide dismutase involves nitration and oxidation of critical tyrosine residues. *Biochemistry* 37: 1613–1622, 1998.
41. Maulik N, Engelman DT, Watanabe M, Engelman RM, Maulik G, Cordis GA, and Das DK. Nitric oxide signaling in ischemic heart. *Cardiovasc Res* 30: 593–601, 1995.
42. Miller FJ, Jr., Gutterman DD, Rios CD, Heistad DD, and Davidson BL. Superoxide production in vascular smooth muscle contributes to oxidative stress and impaired relaxation in atherosclerosis. *Circ Res* 82: 1298–1305, 1998.
43. Moncada S and Higgs A. The L-arginine-nitric oxide pathway. *N Engl J Med* 329: 2002–2012, 1993.
44. Naseem SA, Kontos MC, Rao PS, Jesse RL, Hess ML, and Kukreja RC. Sustained inhibition of nitric oxide by NG-nitro-L-arginine improves myocardial function following ischemia/reperfusion in isolated perfused rat heart. *J Mol Cell Cardiol* 27: 419–426, 1995.
45. Nithipatikom K, Gross ER, Endsley MP, Moore JM, Isbell MA, Falck JR, Campbell WB, and Gross GJ. Inhibition of cytochrome P450omega-hydroxylase: a novel endogenous cardioprotective pathway. *Circ Res* 95: e65–71, 2004.
46. Oyadomari S, Takeda K, Takiguchi M, Gotoh T, Matsumoto M, Wada I, Akira S, Araki E, and Mori M. Nitric oxide-induced apoptosis in pancreatic beta cells is mediated by the endoplasmic reticulum stress pathway. *Proc Natl Acad Sci USA* 98: 10845–10850, 2001.
47. Pandian RP, Parinandi NL, Ilangovan G, Zweier JL, and Kuppusamy P. Novel particulate spin probe for targeted determination of oxygen in cells and tissues. *Free Radic Biol Med* 35: 1138–1148, 2003.
48. Pernow J and Wang QD. The role of the L-arginine/nitric oxide pathway in myocardial ischaemic and reperfusion injury. *Acta Physiol Scand* 167: 151–159, 1999.
49. Petrich BG and Wang Y. Stress-activated MAP kinases in cardiac remodeling and heart failure; new insights from transgenic studies. *Trends Cardiovasc Med* 14: 50–55, 2004.
50. Rajesh KG, Suzuki R, Maeda H, Yamamoto M, Yutong X, and Sasaguri S. Hydrophilic bile salt ursodeoxycholic acid protects myocardium against reperfusion injury in a PI3K/Akt dependent pathway. *J Mol Cell Cardiol* 39: 766–776, 2005.
51. Ray PS, Maulik G, Cordis GA, Bertelli AA, Bertelli A, and Das DK. The red wine antioxidant resveratrol protects isolated rat hearts from ischemia reperfusion injury. *Free Radic Biol Med* 27: 160–169, 1999.
52. Reiter CD, Teng RJ, and Beckman JS. Superoxide reacts with nitric oxide to nitrate tyrosine at physiological pH via peroxynitrite. *J Biol Chem* 275: 32460–32466, 2000.
53. Salloum F, Yin C, Xi L, and Kukreja RC. Sildenafil induces delayed preconditioning through inducible nitric oxide synthase-dependent pathway in mouse heart. *Circ Res* 92: 595–597, 2003.
54. Sato H, Zhao ZQ, and Vinten–Johansen J. L-Arginine inhibits neutrophil adherence and coronary artery dysfunction. *Cardiovasc Res* 31: 63–72, 1996.
55. Seubert J, Yang B, Bradbury JA, Graves J, Degraff LM, Gabel S, Gooch R, Foley J, Newman J, Mao L, Rockman HA, Hammock BD, Murphy E, and Zeldin DC. Enhanced postischemic functional recovery in CYP2J2 transgenic hearts involves mitochondrial ATP-sensitive K+ channels and p42/p44 MAPK pathway. *Circ Res* 95: 506–514, 2004.
56. Shankar RA, Hideg K, Zweier JL, and Kuppusamy P. Targeted antioxidant properties of N-[(tetramethyl-3-pyrroline-3-carboxamido)propyl]phthalimide and its nitroxide metabolite in preventing postischemic myocardial injury. *J Pharmacol Exp Ther* 292: 838–845, 2000.
57. Shinmura K, Tang XL, Takano H, Hill M, and Bolli R. Nitric oxide donors attenuate myocardial stunning in conscious rabbits. *Am J Physiol* 277: H2495–2503, 1999.
58. Shinmura K, Xuan YT, Tang X L, Kodani E, Han H, Zhu Y, and Bolli R. Inducible nitric oxide synthase modulates cyclooxygenase-2 activity in the heart of conscious rabbits during the late phase of ischemic preconditioning. *Circ Res* 90: 602–608, 2002.
59. Toth A, Halmosi R, Kovacs K, Deres P, Kalai T, Hideg K, Toth K, and Sumegi B. Akt activation induced by an antioxidant compound during ischemia-reperfusion. *Free Radic Biol Med* 35: 1051–1063, 2003.
60. Ushmorov A, Ratter F, Lehmann V, Droge W, Schirrmacher V, and Umansky V. Nitric-oxide-induced apoptosis in human leukemic lines requires mitochondrial lipid degradation and cytochrome C release. *Blood* 93: 2342–2352, 1999.
61. Wang Y, Ahmad N, Kudo M, and Ashraf M. Contribution of Akt and endothelial nitric oxide synthase to diazoxide-induced late preconditioning. *Am J Physiol Heart Circ Physiol* 287: H1125–1131, 2004.
62. Wang Y, Guo Y, Zhang SX, Wu WJ, Wang J, Bao W, and Bolli R. Ischemic preconditioning upregulates inducible nitric oxide synthase in cardiac myocyte. *J Mol Cell Cardiol* 34: 5–15, 2002.
63. Weyrich AS, Ma XL, and Lefer AM. The role of L-arginine in ameliorating reperfusion injury after myocardial ischemia in the cat. *Circulation* 86: 279–288, 1992.
64. Woolfson RG, Patel VC, Neild GH, and Yellon DM. Inhibition of nitric oxide synthesis reduces infarct size by an adenosine-dependent mechanism. *Circulation* 91: 1545–1551, 1995.
65. Yoshida T, Watanabe M, Engelman DT, Engelman RM, Schley JA, Maulik N, Ho YS, Oberley TD, and Das DK. Transgenic mice overexpressing glutathione peroxidase are resistant to myocardial ischemia reperfusion injury. *J Mol Cell Cardiol* 28: 1759–1767, 1996.
66. Zhang X, Chen J, Graham SH, Du L, Kochanek PM, Draviam R, Guo F, Nathaniel PD, Szabo C, Watkins SC, and Clark RS. Intranuclear localization of apoptosis-inducing factor (AIF) and large scale DNA fragmentation after traumatic brain injury in rats and in neuronal cultures exposed to peroxynitrite. *J Neurochem* 82: 181–191, 2002.

67. Zhao X, He G, Chen YR, Pandian RP, Kuppusamy P, and Zweier JL. Endothelium-derived nitric oxide regulates postischemic myocardial oxygenation and oxygen consumption by modulation of mitochondrial electron transport. *Circulation* 111: 2966–2972, 2005.
68. Zweier JL, Fertmann J, and Wei G. Nitric oxide and peroxynitrite in postischemic myocardium. *Antioxid Redox Signal* 3: 11–22, 2001.
69. Zweier JL, Wang P, and Kuppusamy P. Direct measurement of nitric oxide generation in the ischemic heart using electron paramagnetic resonance spectroscopy. *J Biol Chem* 270: 304–307, 1995.

Address reprint requests to:
Periannan Kuppusamy, Ph.D.
Davis Heart and Lung Research Institute
The Ohio State University
420 W. 12th Ave, Room 114
Columbus, OH 43210

E-mail: kuppusamy.1@osu.edu

Date of first submission to ARS Central, June 14, 2008; date of final revised submission, October 12, 2008; date of acceptance, October 12, 2008.

This article has been cited by:

1. Yu-Li Pang, Bing-Shuo Chen, Sheng-Ping Li, Chien-Chi Huang, Shih-Wei Chang, Chen-Fuh Lam, Yu-Chuan Tsai. 2012. The preconditioning pulmonary protective effect of volatile isoflurane in acute lung injury is mediated by activation of endogenous iNOS. *Journal of Anesthesia* . [CrossRef]
2. Denis A. Komarov, Ilirian Dhimitruka, Igor A. Kirilyuk, Dmitrii G. Trofimiov, Igor A. Grigor'ev, Jay L. Zweier, Valery V. Khramtsov. 2012. Electron paramagnetic resonance monitoring of ischemia-induced myocardial oxygen depletion and acidosis in isolated rat hearts using soluble paramagnetic probes. *Magnetic Resonance in Medicine* **68**:2, 649-655. [CrossRef]
3. M. Khan, S. Meduru, R. Gogna, E. Madan, L. Citro, M. L. Kuppusamy, M. Sayyid, M. Mostafa, R. L. Hamlin, P. Kuppusamy. 2011. Oxygen cycling in conjunction with stem cell transplantation induces NOS3 expression leading to attenuation of fibrosis and improved cardiac function. *Cardiovascular Research* . [CrossRef]
4. Valery Khramtsov, Denis KomarovNanospin Probes and Applications to Cardiology 200-220. [CrossRef]
5. F. Flachsbart, M. Ufer, R. Kleindorp, S. Nikolaus, S. Schreiber, A. Nebel. 2011. Genetic Variation in the CYP2C Monooxygenase Enzyme Subfamily Shows No Association With Longevity in a German Population. *The Journals of Gerontology Series A: Biological Sciences and Medical Sciences* . [CrossRef]
6. Mahmood Khan, Pawel Kwiatkowski, Brian K. Rivera, Periannan Kuppusamy. 2010. Oxygen and oxygenation in stem-cell therapy for myocardial infarction. *Life Sciences* **87**:9-10, 269-274. [CrossRef]
7. Rizwan Ahmad , Mahmood Khan , Deepti S. Vikram , Anna Bratasz , Periannan Kuppusamy EPR Oximetry: Method and Application 100-110. [Abstract] [Summary] [Full Text PDF] [Full Text PDF with Links]
8. Dipak K. Das Methods in Redox Signaling . [Citation] [Full Text HTML] [Full Text PDF] [Full Text PDF with Links]